CHAPTER 3

FUNDAMENTAL PRINCIPLES OF SOLAR CELL DEVICES

3.1 Introduction

Solar cells are semiconductor devices that convert sunlight directly to electrical energy by using the photovoltaic process. Not only the energy conversion ability of the cell is important, but also the ability of the cell to perform well over a long period of time under changing conditions. In this chapter, starting from the fundamental equations that describe a semiconductor device, solutions are first discussed for the most simple cell model (p-n junction). In this simple model, the ideal and illuminated current-voltage characteristics of a solar cell are obtained. Using this theory, the ideal and illuminated current-voltage (I-V) characteristics of a typical solar cell will be discussed. The output parameters will be defined, and the parameters influencing the conversion efficiencies of photovoltaic devices will finally be outlined.

3.2 Outline of Solar Cell Development

Solar cells depend upon the photovoltaic effect for their operation. Becquerel, who observed a light-dependent voltage between electrodes immersed in an electrolyte, reported this effect initially in 1839. It was also observed in an all-solid-state system in 1876 for the case of selenium. This was followed by the development of photocells based on both this material and cuprous oxide. Although a silicon cell was reported in 1941, it was not until 1954 that the forerunner of present silicon cells was announced.

This device represented a major development because it was the first photovoltaic structure that converted light to electricity with reasonable efficiency. These cells found application as power sources in spacecrafts as early as 1958. By the early 1960's, the design of cells for space use had stabilized and over the next decade this was their major application.

The early 1970's saw an innovative period in silicon cell development with marked increases in realizable energy-conversion efficiencies. At about the same time, there was a reawakening of interest in terrestrial use of these devices. By the end of the 1970's, the volume of cells produced for terrestrial use had completely outstripped that for space use. This increase in production volume was accompanied by a significant reduction in solar cell costs. The early 1980's saw newer device technologies being evaluated at the pilot production stage, poised to enable further reduction in costs over the coming decade. With such cost reductions a continual expansion of the range of commercial applications was ensured for this approach to utilize the sun's energy.

3.3 p-n Junction Diodes

3.3.1 Introduction

The most common configuration of a solar cell is a p-n junction. A p-n junction is a device made of two zones with different doping, one of p-type (holes as majority carriers) and the other n-type (electrons as majority carriers). It is assumed that these doped regions are uniformly doped and that the transition between the two regions is to be an abrupt p-n junction.

3.3.2 Electrostatic analysis of a p-n junction

The electrostatic analysis of a p-n junction is of interest since it provides knowledge about the charge density and the electric field in the depletion region. Suppose that these two semiconductors with different vacuum energy (defined as the energy of an electron at rest just outside the crystal and not interacting with it) approach each other (see Fig. 3.1). Before electrical contact is made, the n-type region has an excess of electrons with respect to the p-region and the p-region has an excess of holes with respect to the n-region. After contact, a gradient of concentration of carriers at the junction exist and an equilibrium state is subsequently established.

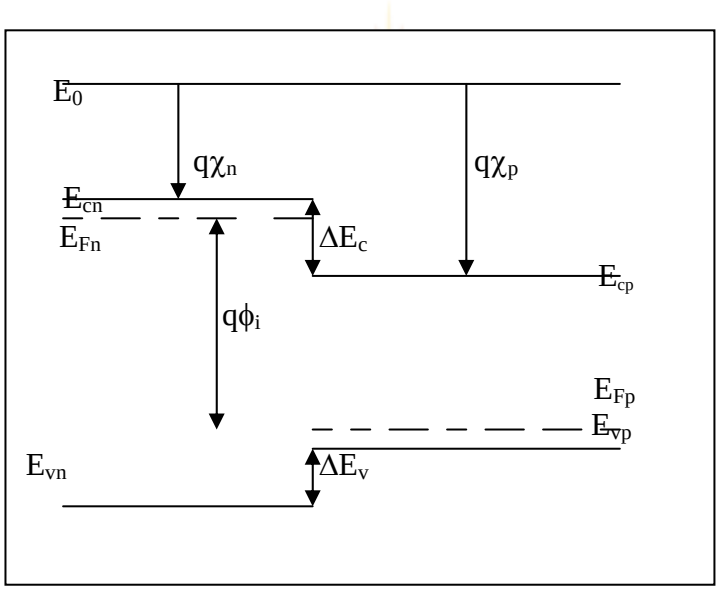

Figure 3.1: Flat band energy diagram of a p-n junction before the merging of n-type and p-type regions.

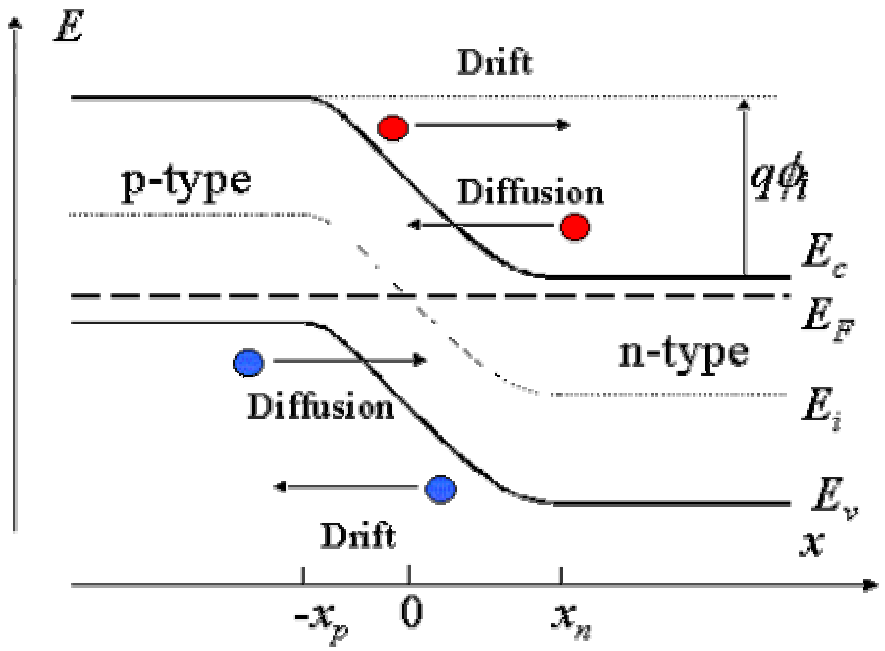

Figure 3.2: Energy band diagram of a typical p-n junction in thermal equilibrium.

To reach thermal equilibrium, electrons/holes close to the metallurgical junction diffuse across the junction into the p-type/n-type region where hardly any electrons/holes are present. This process leaves the ionized donors (acceptors) behind, creating a region around the junction, which is depleted of mobile carriers. We call this region the depletion region. The charge due to the ionized donors and acceptors causes an electric field, which in turn causes drift of carriers in the opposite direction. The diffusion of carriers continues until the drift current balances the diffusion current, thereby reaching the thermal equilibrium as indicated by a constant Fermi energy [Schockley, 1950; Streetman, 1990; Lindmayer and Wrigley, 1965 and Sze, 1981]. When the junction is in equilibrium as shown in Figure (3.2), the energy barrier between n and p zones is $q\phi_i$ (where ϕ_i is the diffusion potential and q the electric charge).

3.3.3 Calculation of the contact potential (built-in voltage)

The built-in potential in a semiconductor equals the potential across the depletion region in thermal equilibrium. Since thermal equilibrium implies that the Fermi energy is constant throughout the p-n junction, the built-in potential equals the difference in the Fermi energies, $E_{F,n}$ and $E_{F,p}$, divided by the electronic charge. From the energy diagram in Fig. 3.1 it is found:

$$q\phi_i = E_{F,n} - E_{F,p} = E_{F,n} - E_{c,n} + E_{c,n} - E_{c,p} + E_{c,p} - E_{F,p} \tag{3.1}$$

This can be expressed as a function of the electron concentrations and the effective densities of states in the conduction band:

$$q\phi_i = \Delta E_c + kT \ln\left(\frac{n_{no} N_{c,p}}{n_{po} N_{c,n}}\right) \tag{3.2}$$

where $N_{c,p}$ and $N_{c,n}$ are the effective densities of states at the conduction band edge of p and n regions respectively, n_{p0} and n_{n0} indicate the equilibrium concentration of electrons on the p-side and n-side respectively.

The built-in voltage can also be related to the hole concentrations and the effective density of states of the valence band:

$$q\phi_i = -\Delta E_v + kT \ln\left(\frac{p_{po} N_{v,n}}{p_{no} N_{v,p}}\right) \tag{3.3}$$

where $N_{v,p}$ and $N_{v,n}$ are the effective densities of states at the valence band edge for p and n regions respectively, p_{p0} and p_{n0} are the equilibrium concentration of holes on the p-side and n-side respectively,

The intrinsic carrier concentration of a semiconductor is given by:

$$n_{i,n}{}^2 = N_{c,n}N_{v,n}\exp\left(-\frac{E_{v,n}-E_{c,n}}{kT}\right) \tag{3.4a}$$

and

$$n_{i,p}{}^2 = N_{c,p}N_{v,p}\exp\left(-\frac{E_{v,p}-E_{c,p}}{kT}\right) \tag{3.4b}$$

Combining above expressions yield the built-in voltage independent of the free carrier concentrations:

$$q\phi_i = \frac{\Delta E_c - \Delta E_v}{2} + kT\ln\frac{N_d N_a}{n_{i,n}n_{i,p}} + \frac{kT}{2}\ln\left(\frac{N_{v,n}N_{c,p}}{N_{c,n}N_{v,p}}\right) \tag{3.5}$$

where $n_{i,n}$ and $n_{i,p}$ are the intrinsic carrier concentrations of the n and p-type region, respectively, N_a and N_d are the acceptor and donor densities respectively. ΔE_c and ΔE_v are the positive quantities if the band gap of the n-type region is smaller than that of the p-type region and the sum of both equals the band gap difference. The above expression reduces to that of the built-in junction of a homojunction if the material parameters in the n-type region equal those in the p-type region. If the effective densities of states are the same the expression reduces to:

$$q\phi_i = \frac{\Delta E_c - \Delta E_v}{2} + kT\ln\left(\frac{N_d N_a}{n_{i,n}n_{i,p}}\right) \tag{3.6}$$

An applied voltage, V_a, will change the potential difference between the two sides of the diodes by V_a. Hence, the potential across the transition region will become ($\phi_i \pm V_a$).

3.3.4 Abrupt p-n junction

For the calculations of the charge, field and potential distribution in an abrupt p-n junction the same approach as for the homojunction is followed. First of all we use the depletion approximation and solve Poisson's equation. The depletion approximation assumes that the depletion region around the metallurgical neutral region has well-defined edges. It also assumes that the transition between the depleted and the quasi-neutral region is abrupt. The quasi-neutral region is defined as the region adjacent to the depletion region where the electric field is small and the free carrier density is close to the net doping density. The depletion approximation is justified by the fact that the carrier densities change exponentially with the position of the Fermi energy relative to band edges. Once the depletion approximation is made it is easy to find the charge profile. It equals the sum of the charges due to the holes, electrons, ionized acceptors and ionized donors:

$$\rho = q(p - n + N_d^+ - N_a^-) \tag{3.7}$$

where it is assumed that no free carriers are present within the depletion region. The electric field is obtained from the charge density using Gauss's law, which states that the field gradient is equal to the charge density divided by the dielectric constant:

$$\frac{d\xi(x)}{dx} = \frac{\rho(x)}{\varepsilon} \tag{3.8}$$

The electric field is obtained by integrating equation (3.8). The boundary conditions consistent with the depletion approximation are that the electric field is zero at both edges of the depletion region, since any field would cause the free carriers to move thereby eliminating the electric field [Schockley, 1961]. The space charge density, electric field strength and the corresponding potential distribution of the p-n junction are

given in Fig. 3.3. An easy way to derive the depletion layer widths in a p-n diode is to treat it as a combination of two schottky diodes, one with an n-type semiconductor and another with a p-type semiconductor. The metal between the two semiconductors is assumed to be infinitely thin. The potential difference between the two semiconductors can then be expressed as:

$$\phi_n + \phi_p = \phi_i - V_a = \frac{1}{q}[E_i - E_{F,p} - (E_i - E_{F,n})] - V_a \quad \text{or}$$

$$= kT\ln[\frac{N_d N_a}{n_i^2}] - V_a \tag{3.9}$$

where ϕ_n and ϕ_p are the potential across the n and p-type materials respectively. These potentials can be expressed as a function of the depletion layer widths just like for the schottky barrier diode, assuming the depletion approximation.

$$\phi_n = \frac{qN_d x_n^2}{2\varepsilon_{s,n}} \text{ and } \phi_p = \frac{qN_a x_p^2}{2\varepsilon_{s,p}} \tag{3.10}$$

To solve equations (3.9) and (3.10) an additional relation between x_n and x_p is obtained by realizing that the positive charge in the n-type semiconductor equals the negative charge in the p-type semiconductor, again assuming the depletion approximation.

$$qN_a x_p = qN_d x_n \tag{3.11}$$

Solving for x_n and x_p yields:

$$x_d = x_n + x_p = \left[\frac{2\varepsilon_{s,n}\varepsilon_{s,p}}{q}\frac{(N_a + N_d)^2(\phi_i - V_a)}{N_a N_d (N_a\varepsilon_{s,p} + N_d\varepsilon_{s,n})}\right]^{\frac{1}{2}} \tag{3.12}$$

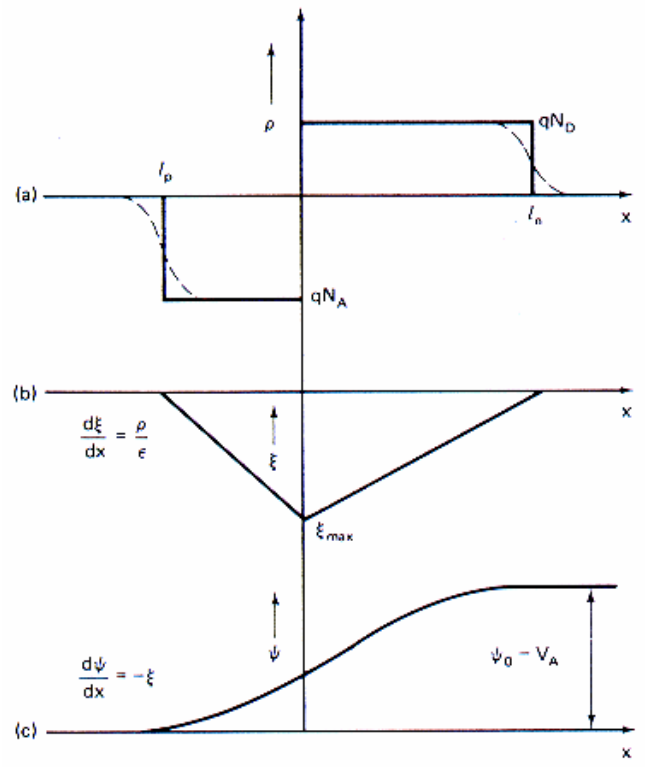

Figure 3.3: (a) Space charge density. The dashed line shows the actual distribution while the solid line shows the assumed distribution in the depletion approximation, (b) corresponding electrical field strength and (c) corresponding potential distribution [Green, 1982].

3.3.5 Current-voltage characteristics

For the derivation of the ideal diode equation it is again assumed that the quasi-Fermi levels are constant throughout the depletion region. In the case of quasi-equilibrium the carrier concentration densities and electrostatic potentials at different points are related by equations:

$$n_{p0} = n_{n0} \exp\frac{-q\phi_i}{kT} \tag{3.13a}$$

$$p_{p0} = p_{n0} \exp\frac{-q\phi_i}{kT} \tag{3.13b}$$

Figure (3.4) depicts the electron and hole concentrations across the p-n junction. The electron concentration at $-x_p$ and x_p are related by: (a similar concentration treatment holds for holes).

$$n(-x_p) = n(x_p)\exp\frac{-q(\phi_i - V_a)}{kT} \tag{3.14}$$

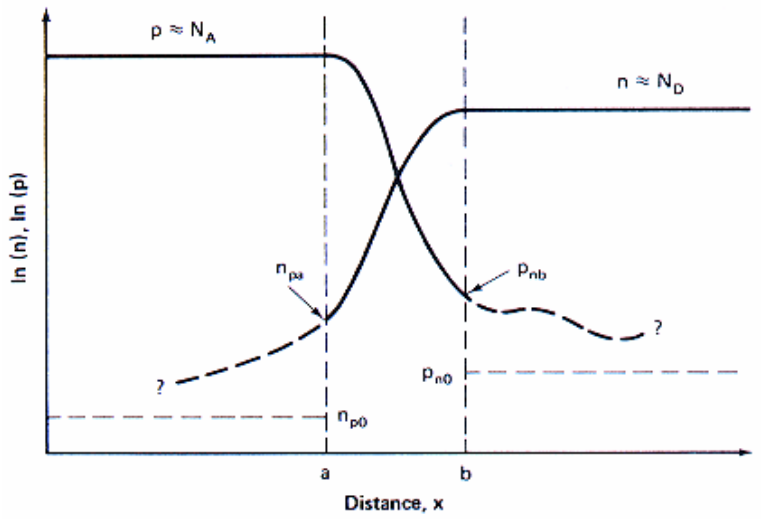

Figure 3.4: Plot of carrier concentrations when a voltage is applied to the p-n junction. In the text, expressions are found for the minority carrier concentrations n_{pa} and p_{nb} at the edge of the junction depletion region. Subsequently, the precise form of the distributions shown dashed are calculated [Green, 1982].

It is reasonable to assume the low-injection condition, i.e. the number of the majority carrier concentrations are changed by a negligible amount at the boundary of the neutral regions; in other words we can put $n(x_p) = n_{n0}$ in equation (3.14). We have

$$n(-x_p) = n_{n0}\exp\frac{-q(\phi_i - V_a)}{kT} = n_{p0}\exp\frac{qV_a}{kT}, \tag{3.15}$$

where use has been made of equation (3.13a). We thus see that the minority carrier (electrons) concentration at the left end of the depletion layer is controlled by the factor exp (qV_a / kT). In the forward bias condition we have injection of minority carriers, while extraction occurs in the reverse bias condition. The change $\Delta n_p(-x_p)$ in electron concentration at the end of the depletion layer (in the p-side part of the semiconductor) is:

$$\Delta n_p(-x_p) = n_{p0}(\exp\frac{qV_a}{kT} - 1) \tag{3.16}$$

For $x < -x_p$ the semiconductor is (approximately) neutral; the excess (or deficit) of minority carriers $\Delta n_p(-x_p)$ gives rise to a diffusion electron current at $x = -x_p$ and is given by:

$$J_n^{(diff)}(-x_p) = qD_n \frac{\Delta n_p(-x_p)}{L_n} = \frac{qD_n n_{p0}}{L_n}(\exp\frac{qV_a}{kT} - 1) \tag{3.17}$$

The total electron current at the boundary $x = -x_p$ is the sum of the diffusion component and drift component, the latter is negligible, because so is the concentration of minority carriers as well as the electric field in the quasi-neutral region $x < -x_p$. We thus have:

$$J_n(-x_p) \cong J_n^{(diff)}(-x_p) = qD_n \frac{\Delta n_p(-x_p)}{L_n} = \frac{qD_n n_{p0}}{L_n}(\exp\frac{qV_a}{kT} - 1) \tag{3.18a}$$

Similarly, for the hole current density on the right boundary ($x = x_n$) of the space-charge region it's obtained that:

$$J_p(x_n) \cong J_p^{(diff)}(x_n) = qD_p \frac{\Delta n_n(x_n)}{L_p} = \frac{qD_p p_{n0}}{L_p}(\exp\frac{qV_a}{kT} - 1) \tag{3.18b}$$

The space charge region is so narrow that we can reasonably assume that the net balance of generation and recombination processes vanishes within it. In this case

electron and hole currents are constant throughout the depletion layer, and the total current through the diode is given by the sum of the contributions of equations (3.18). It follows that

$$J = J_s(\exp\frac{qV_a}{kT} - 1) \tag{3.19a}$$

and

$$J_s = qD_p\frac{p_{n0}}{L_p} + qD_n\frac{n_{p0}}{L_n} = qL_p\frac{p_{n0}}{\tau_p} + qL_n\frac{n_{p0}}{\tau_n} \tag{3.19b}$$

where D_n and D_p are the diffusion coefficients for electrons and holes, τ_n and τ_p are the minority carrier lifetimes for electrons and holes, p_{n0} and n_{p0} are the carrier concentrations at equilibrium, L_p and L_n are the diffusion lengths of the holes and electrons.

3.3.6 Recombination/generation in the depletion region

Recombination/generation currents in a heterojunction can be much more important than in a homojuntion because most recombination/generation mechanisms depend on the intrinsic carrier concentration which depends strongly on the energy band gap. We will only consider two major mechanisms: band-to-band recombination and Schockley-Hall-Read recombination, which are relevant to the operation of Cu(In,Ga)Se_2/ZnO heterojunction devices.

3.3.6.1 Band-to-band recombination

Band-to-band recombination applies to the simple case where an electron-hole pair recombines. An electron occupying a higher energy state undergoes transition from the

conduction band to the valence band by emission of a photon or by transferring the energy to another free electron or hole in the auger process (Fig. 3.5).

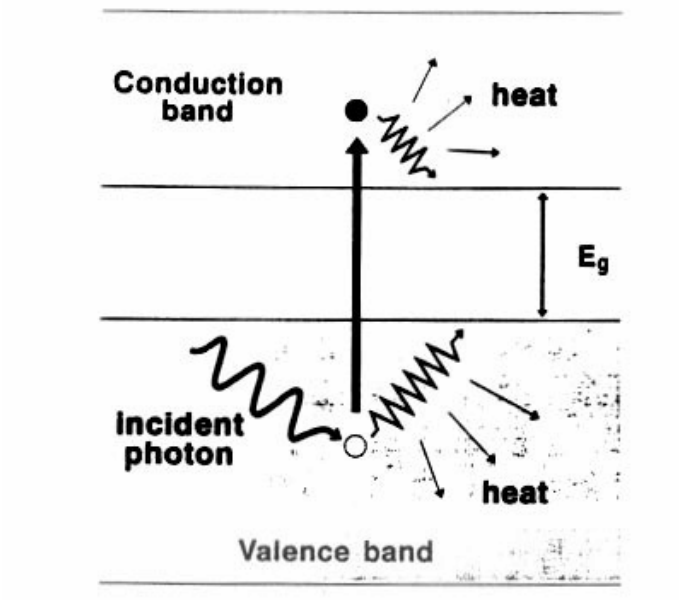

Figure 3.5: One of the major loss mechanisms in solar cells. An electron-hole pair created by a high-energy photon quickly "thermalizes" or relaxes back to the edges of the respective carrier bands. The energy wasted is dissipated as heat [Green, 1982].

The recombination/generation rate due to band-to-band transitions is given by

$$U_{b-b} = b(np - n_i^2) \tag{3.20}$$

where b is the bi-molecular recombination rate. For $np > n_i^2$ (or under forward bias conditions) recombinations dominate, whereas for $np < n_i^2$ (under reverse bias conditions) thermal generations of electron hole pairs occur. Assuming constant quasi-

Fermi levels in the depletion region this rate can be expressed as a function of the applied voltage by using the "modified" mass-action law $np = n_i^2 \exp\frac{qV_a}{kT}$, yielding:

$$U_{b-b} = bn_i^2(\exp\frac{qV_a}{kT} - 1) \tag{3.21}$$

The current is then obtained by integrating the recombination rate throughout the depletion region:

$$J_{b-b} = q\int_{x_n}^{x_p} U_{b-b}\,dx \tag{3.22}$$

For a uniform material (homojunction) this integration yields:

$$J_{b-b} = qbn_i^2(\exp\frac{qV_a}{kT} - 1)x_d \tag{3.23}$$

Whereas for a p-n heterojunction consisting of two uniformly doped regions with different band gap, the integration becomes:

$$J_{b-b} = qb(n_{i,n}^2 x_n + n_{i,p}^2 x_p)(\exp\frac{qV_a}{kT} - 1) \tag{3.24}$$

3.3.6.2 Schockley-Hall-Read recombination

Imperfections and impurities in the semiconductors can introduce energy levels in the forbidden gap. These intermediate levels allow two-step recombination processes in such a way that electrons relax from conduction band energies to the defect level and then proceed on to the valence band annihilating a hole [Schockley and Read, 1952; Hall, 1952 and Hovel, 1975]. Probability of transition depends on the position of the energy level in the gap and the defect density. Recently, recombination in the space

charge region via states in band tails was identified as the dominant bucking current mechanism in Cu(In,Ga)Se_2/ZnO devices [Klenk and Schock, 1994]. Provided bias conditions are “close” to thermal equilibrium the recombination rate due to a density, N_t, of traps with energy, E_t, and a recombination cross-section σ is given by:

$$U_{SHR} = \frac{np - n_i^2}{n + p + 2n_i \cosh\frac{E_i - E_t}{kT}} N_t \sigma \upsilon_{th} \tag{3.25}$$

where n_i is the intrinsic carrier concentration, υ_{th} is the thermal velocity of the carriers and E_i is the intrinsic energy level. For $E_i = E_t$ and $\tau_0 = \frac{1}{N_t \sigma \upsilon_{th}}$

$$U_{SHR} = \frac{np - n_i^2}{n + p + 2n_i} \frac{1}{\tau_0} \tag{3.26}$$

Throughout the depletion region the product of electron and hole density is given by the “modified” mass action law:

$$np = n_i^2 (\exp\frac{qV_a}{2kT} - 1) \tag{3.27}$$

This enables to find the maximum recombination rate that occurs for $n = p = n_i \exp\frac{qV_a}{2kT}$

$$U_{SHR,\max} = \frac{n_i}{2\tau_0} (\exp\frac{qV_a}{2kT} - 1) \tag{3.28}$$

The total recombination current is obtained by integrating the recombination rate over the depletion layer width:

$$\Delta J_n = -\Delta J_p = q \int_{-x_p}^{x_n} U_{SHR} dx \tag{3.29}$$

which can be written as a function of the maximum recombination rate and an “effective” width x':

$$\Delta J_n = qU_{SHR,\max} x' = q\frac{x' n_i}{2\tau_0}(\exp\frac{qV_a}{2kT} - 1) \tag{3.30}$$

where
$$x' = \frac{\int_{-x_p}^{x_n} U_{SHR}\, dx}{U_{SHR,\max}} \tag{3.31}$$

Since $U_{SHR,\max}$ is larger than, or equal to U_{SHR} anywhere within the depletion layer one finds that x' has to be smaller than $x_d = x_n + x_p$. The calculation of x' requires a numerical integration. Substituting equations (3.4a) and (3.4b) into equation (3.31) then yields x'.

3.3.7 The illuminated I-V curve

Under light radiation when the junction is illuminated by photons whose energy is higher than the energy gap, electron-hole pairs are created. The minority carriers are subsequently pushed down to the energy barrier of the intrinsic field. The result is the separation of the generated electrons from the holes into the p-n junction. These carriers generate a field which is opposite to the intrinsic electric field ξ', so that the resulting total electric field is given by $\xi - \xi'$. There is then a voltage at open circuit V in the direction of direct polarization into the illuminated region. This effect is called the photovoltaic effect. Consider a situation of non-equilibrium, starting from the general one-dimensional transport equations:

$$\frac{\partial n}{\partial t} = D_n \frac{\partial^2 n}{\partial x^2} + \mu_n \varepsilon \frac{\partial n}{\partial x} + \mu_n n \frac{\partial \xi}{\partial x} - \frac{(n - n_0)}{\tau_n} + G_n(x) \tag{3.32a}$$

$$\frac{\partial p}{\partial t} = D_p \frac{\partial^2 p}{\partial x^2} + \mu_p \varepsilon \frac{\partial p}{\partial x} + \mu_p p \frac{\partial \xi}{\partial x} - \frac{(p - p_0)}{\tau_p} + G_p(x), \tag{3.32b}$$

where G_n and G_p are electron and hole generation rates respectively. Then solving these equations for solar cells it must be considered that the generation of electrons and holes are identical. Moreover, there can be either $p >> n$ or $n >> p$, so that equations (3.32a) and (3.32b) are uncoupled and the term $\frac{\partial \xi}{\partial x}$ is neglected [Fahrenbruch and Bube, 1983]. Finally considering steady state conditions (compared with carrier lifetimes) $\frac{dp}{dt} = 0$ or $\frac{dn}{dt} = 0$ and a single transport equation suffices to describe the excess of minority carrier density:

$$D_p \frac{\partial^2 p_n}{\partial x^2} + \mu_p \varepsilon \frac{\partial p_n}{\partial x} - \frac{(p_n - p_{n0})}{\tau_p} + G(x) = 0 \qquad (3.33)$$

This equation gives the current density of a part of the semiconductor (in this case the p-doped part). Taking into account the condition of constant generation rate G through out the cell and considering only the minority carriers in depletion approximation, it is obtained that:

$$p(x) - p_0 = C \exp \frac{-(x - x_n)}{L_p} + G\tau_p \qquad (3.34)$$

and the general dependence of the total diode current density can be expressed as;

$$J = J_s(\exp \frac{qV_t}{kT} - 1) - J_L , \qquad (3.35)$$

where $J_L = qG(W + L_p + L_n)$ is the light-generated current density, W the width of the depletion region and J_s is the saturated current density.

The expression for total current density will be used to quantify the performance of heterojunction devices in chapter 5. This equation is just an approximation of the real situation but gives a very clear picture of the behaviour of the photo generator device,

and shows how the dependence of the current (I) on the voltage (V) is expressed (see Fig. 3.6).

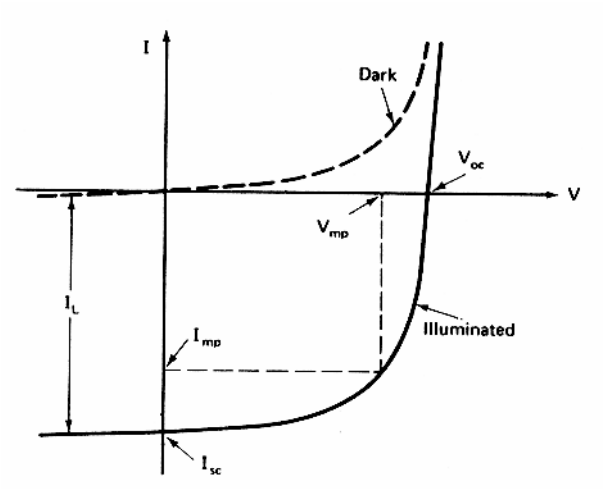

Figure 3.6: Terminal properties of a p-n junction diode in the dark and when illuminated [Green, 1982].

3.4 Solar Cell Output Parameters

Three important parameters that are usually used to characterize solar cell outputs are *the short-circuit current*, I_{SC}, *the open-circuit voltage*, V_{OC}, and *the fill factor, FF*. The short-circuit current, I_{SC}, under ideal conditions, is equal to the light-generated current I_L. An expression for an ideal value for the open-circuit voltage, V_{OC}, is obtained by setting the total current, I, to zero in equation (3.35) and then the following equation will result:

$$V_{OC} = \frac{kT}{q}\ln(\frac{I_L}{I_S} + 1) \qquad (3.36)$$

V_{OC} is determined by the properties of the semiconductor by virtue of its dependence on I_{SC}. The power output for any operating point on the I-V curve is computed from the area of the rectangle indicated in the fourth quadrant indicated in Fig. 3.6. One

particular operating point (V_{mp}, I_{mp}) will maximize this power output. The third parameter, the fill factor, FF, is defined as;

$$FF = \frac{V_{mp} I_{mp}}{V_{oc} I_{sc}} \tag{3.37}$$

It is a measure of the "squareness" of the output characteristics of the cell. For cells of reasonably efficiency it has a value in the range of 0.7 to 0.85. The energy-conversion efficiency, η, is then given by:

$$\eta = \frac{V_{mp} I_{mp}}{P_{in}} = \frac{V_{oc} I_{sc} FF}{P_{in}} \tag{3.38}$$

where P_{in} is the total power in the light incident upon the cell, and is given by:

$$P_{in} = A\int_0^\infty F(\lambda)(hc/\lambda)d\lambda \tag{3-39}$$

Here A is the device area, $F(\lambda)$ is the number of photons per square centimeter per second per unit bandwidth incident on the device at wavelength λ, and hc/λ is the energy of each photon. Energy-conversion efficiencies of commercial solar cells generally lie in the 12 - 14% range.

3.5 Efficiency Limits and Losses

3.5.1 Short-circuit current

Under ideal conditions, each photon incident on the cell of greater energy than that of the band gap gives rise to one electron flowing in the external circuit. Hence, to calculate the maximum short-circuit current, I_{SC}, the photon flux in sunlight must be known. This can be calculated from the energy distribution of sunlight by dividing the energy content at a given wavelength by the energy of an individual photon (hf

or hc/λ) of this wavelength. The maximum I_{SC} is then found by integrating these distributions from low wavelengths up to the maximum wavelength for which electron-hole pairs can be generated for a given semiconductor. Three types of losses in solar cells can be described by being of an optical nature. These are:

(i) The reflectiveness of the material. To reduce this, an anti-reflective (AR) coating (MgF_2 in the case of CIS-based cells) is used in some applications,

(ii) The front contact (to the side of the cell exposed to the sunlight) blocks 5-10% of the incoming sunlight, and

(iii) If the cell is not thick enough, some of the light will pass right through before being absorbed. This problem is not significant for direct-band gap materials like $Cu(In,Ga)Se_2$.

Because of the wavelength dependence of the absorption coefficient, it is expected that the shorter wavelength photons will be absorbed close to the surface, while the longer wavelengths are absorbed deep in the bulk. Surface recombination will therefore be more important for short wavelengths while recombination in the quasi-neutral region is more important for long wavelengths. Short circuit current losses can also occur due to recombination at the surfaces and/or in the bulk of semiconductor materials. Only electron-hole pairs generated near the p-n junction contribute towards I_{SC}.

3.5.2 Open-circuit voltage and efficiency of solar cell

The open circuit voltage, V_{OC}, can be simplified further for $I_L / I_S >> 1$ as:

$$V_{OC} = \frac{kT}{Aq}\ln\left(\frac{I_L}{I_S}+1\right) \approx \frac{kT}{Aq}\ln\frac{I_L}{I_S} \tag{3.40}$$

For good performance, I_L and V_{OC} must be as large as possible. The maximum value of I_L would be obtained if all photo generated electron-hole pairs are collected as photocurrent, and I_L can achieve 80-90% of this limit if light absorption and minority carrier collection are both highly efficient. The limiting value of V_{OC} is the built-in voltage ϕ_i, corresponding to complete flattening of the bands across the junction. This could only happen under extremely intense illumination and 1 sun V_{OC} is usually no more than approximately $0.7\phi_i$. Inspection of equation (3.40) shows that V_{OC} increases as the saturation current I_S decreases. Interestingly, I_S has no absolute minimum value. In thin film solar cells with well-passivated surfaces, I_S can be reduced to zero and V_{OC} increase towards its upper limit of ϕ_i. In thicker cells in which volume recombination occurs, the lower limit on I_S is determined by the rate of radiative recombination of minority carriers. Usually non-radiative recombination also occurs and this raises I_S by some orders of magnitude and lowers V_{OC} accordingly. When recombination in the transition region is not ignored an additional term must be added to the current-voltage characteristics and then equation (3.19a) becomes

$$I = I_0[\exp\frac{qV_a}{kT} - 1] + I_w[\exp\frac{qV_a}{2kT} - 1] \qquad (3.41)$$

where I_W has the value [Sah, 1957]

$$I_w = \frac{qAn_i\pi}{2\tau_n\tau_p} x \frac{kT}{q\xi_{\max}}$$

where $\xi_{\max}$ is the maximum electric field strength in the junction, τ_n and τ_p are the minority carrier lifetimes for electrons and holes.

The second term of this expression dominates at low currents while the first term dominates at high currents.

3.5.3 Fill factor (*FF*)

An empirical expression for the fill factor [Green, 1982], which is accurate up to four digits for $\nu_{oc} > 10$ is given by;

$$FF_o = \frac{\upsilon_{oc} - \ln(\upsilon_{oc} + 0.72)}{\upsilon_{oc} + 1} \qquad 3.42)$$

where ν_{oc} is a normalized voltage and defined as:

$$\upsilon_{oc} = \frac{qV_{oc}}{AkT}$$

Generally, solar cells have finite series resistance, R_S, due to the bulk resistance of the semiconductor materials, the contact resistance between the metallic contacts and the semiconductor and the resistance of the metallic contacts itself. The leakage current across the p-n junction around the edge of the cell occurs due to the presence of the defects and is described in terms of a shunt resistance, R_{SH}. Both the series and the shunt resistance reduce the fill factor because of the influence on I_{SC} and V_{OC}. The magnitude of this reduction can be found by defining the characteristic resistance, R_{ch}, of a solar cell to be [Green, 1977]:

$$R_{ch} = \frac{V_{OC}}{I_{SC}} \qquad (3.43)$$

If $R_S << R_{ch}$ or $R_{SH} >> R_{ch}$, the effect on fill factor will be minimum. Defining a term called the normalized series resistance, r_s, as:

$$r_s = \frac{R_S}{R_{ch}}$$

an approximated expression for the fill factor becomes:

$$FF = FF_o(1 - r_s) \tag{3.44}$$

Equation (3.44) is accurate up to two significant digits for v_{oc} > 10 and r_s < 0.4. A normalized shunt resistance, r_{sh}, is now also defined as:

$$r_{sh} = \frac{R_{SH}}{R_{ch}}$$

A corresponding expression for the effect of shunt resistance on fill factor is [Green, 1982];

$$FF = FF_o[1 - \frac{(v_{oc} + 0.7)}{v_{0c}} x \frac{FF_o}{r_{sh}}] \tag{3.45}$$

Equation (3.45) is accurate to close to three significant digits for v_{oc} > 10 and r_{sh} < 2.5. When a situation arises where both series and shunt resistance play a role, equations (3.44) and (3.45) can be combined (FF_o in equation (3.45) is equal to FF in equation (3.44)) such that

$$FF = FF_o(1 - r_s)[1 - \frac{(\upsilon_{oc} + 0.7)}{\upsilon_{oc}} x \frac{FF_o(1 - r_s)}{r_{sh}}] \tag{3.46}$$

The description of CIS and related compound solar cells in terms of equation (3.46) works reasonably well. For example, the world record cell has a fill factor of 78.6% and the value calculated from equation (3.46) is 78% [Contreras et al., 1999].

3.6 Voltage Dependence of the Light Generated Currents

As the band gap of $CuInSe_2$ is increased by alloying with Ga or S, the loss in efficiency due to the decrease of light generated current with increasing voltage becomes important. The voltage dependence of the light generated currents can be determined by analysis of the current-voltage (I-V) measurements made at two different light intensities. By adding an I-V measurement at a third light intensity it is possible also to determine if the analysis technique is valid. It has been demonstrated that the loss in efficiency of $Cu(InGa)Se_2$ solar cells with high Ga content is due to decrease in the fill factor, and to a lesser extent V_{OC} which is caused by a drop in the light generated current with increasing forward voltage [Shafarman et al, 1996a; Shafarman et al., 1996b].

References

Contreras M. A., Egaas B., Ramanathan K., Hiltner J., Swartzlander A., Hasoon F. and Noufi R., *Prog. Photovoltaic Res. Appl*. **7**, pp. 311-316, (1999).

Fahrenbruch A. L. and Bube H., Fundamentals of Solar Cells, Academic Press, London, (1983).

Green M. A., *Solid State Electronics* **20**, pp. 265-266, (1977).

Green M. A., Solar Cells, Prentice-Hall, New York, (1982).

Hall R. N., *Phys. Rev*. **8**, p. 387, (1952).

Hovel H. J., 10th IEEE Photovoltaic Specialist Conf., Palo Alto, pp. 34-39, (1975).

Klenk R. and Schock H. W., Proc. 12th European Photovoltaic Solar Energy Conf., Amsterdam, H. S. Stephens and Associates, Bedford, (1994).

Lindmayer J. and Wrigley C. Y., Fundamentals of Semiconductor Devices, Princeton, NJ: Van Nostrand, (1965).

Sah C. T., *Proceedings of the IRE* **45**, pp. 1228-1243, (1957).

Schockely W., Electrons and Holes in Semiconductors, Princeton, NJ: van Nostrand, (1950).

Schockley W. and Queisser H. J., *Journal of Applied Physics* **32**, pp. 510-519, (1961).

Schockley W. and Read W. T., Jr, *Phys. Rev*. **87**, p. 835, (1952).

Shafarman W. N., Klenk R. and McCandless B. E., In Proc. Of 25th IEEE PVSC, p. 763, (1996a).

Shafarman W. N., Klenk R. and McCandless B. E., *J. Appl. Phys*. **79**(9), p. 7324, (1996b)

Streetman B. G., Solid State Electronic Devices, 3rd ed. Englewood Cliffs, NJ: Prentice Hall, (1990).

Sze S. M., Physics of Semiconductor Devices, Wiley, New York, (1981).